Environmental Science Nano

ROYAL SOCIETY OF CHEMISTRY

PAPER

View Article Online
View Journal | View Issue

Cite this: *Environ. Sci.: Nano*, 2021, **8**, 3015

Phytotoxicity of halloysite nanotubes using wheat as a model: seed germination and growth†

Linhong Chen,‡[a] Zizheng Guo,‡[b] Biyin Lao,[a] Chunlei Li,[b] Jianhua Zhu,*[b] Rongmin Yu [b] and Mingxian Liu *[a]

Received 4th June 2021,
Accepted 18th August 2021

DOI: 10.1039/d1en00507c

rsc.li/es-nano

Due to their special structure and biocompatibility, halloysite nanotubes (HNTs) have critical applications in polymer composites, drug delivery, waste treatment, and cosmetics. With the advance of industrial products based on HNTs and agrochemical carriers, it is urgent to study their phytotoxicity. Here, the influence of HNTs on the germination and growth of plants using wheat seeds as a model was investigated. The biomass, chlorophyll content and oxidative damage index of the HNT treated wheat group were compared with the control. HNTs have no significant effect on the germination of wheat seeds. The biomass (root/shoot length, and fresh weight) of the wheat treated with different concentrations of HNTs increased at doses of 0.1, 1, and 10 mg mL^{-1}, while it decreased significantly at high concentrations of HNTs (100 mg mL^{-1}). The chlorophyll content and oxidative damage index (cell membrane permeability, H_2O_2 content, malondialdehyde content) increased with HNT concentration. A large accumulation of HNTs on the root sections was found in the high concentration HNT group, while no HNTs were observed in the xylem. Furthermore, HNTs can slightly decrease the viability of tobacco cells and promote the accumulation of biomass and secondary metabolites. This work demonstrated that HNTs at a certain concentration are safe to plants, while they are harmful at a high dose of 100 mg mL^{-1}. The understanding of the phytotoxicity of HNTs is helpful for their applications in the environmental protection and agricultural field.

Environmental significance

Soil pollution is one of the three major pollution factors in the world. The wide use of clay nanomaterials leads to an increasing release in the environment. It is urgent to figure out the phytotoxicity of a widely used natural tubular mineral, *i.e.* halloysite nanotubes (HNTs). Their industrial products have developed rapidly because of their good comprehensive properties. It was found that HNTs could enter the plant roots and promote wheat growth, while they improved the accumulation of biomass and secondary metabolites of tobacco cells. These findings are significant for developing HNT application in environmental protection such as waste treatment, as well as their potential in controlling pesticide or fertilizer release.

1. Introduction

Nanoparticles have been widely used in composites, biomedicine, cosmetics, and other commercial fields in daily life. Recently, emerging applications of nanoparticles in agriculture have been developed, which can provide innovative solutions to promote food production and quality and lower the consumption of pesticides and fertilizers.[1] Maize seed treatment and foliar spraying of Zn–chitosan nanoparticles (0.01–0.16%) significantly controlled *Curvularia* leaf spot and increased grain yield.[2] Urea–hydroxyapatite nanohybrids were also synthesized by a one-pot synthesis method, which was used to release nitrogen slowly.[3] Initial trials on rice farms revealed that hybrid rice can save up to 50% in urea consumption, demonstrating that slow-release fertilizers could significantly reduce the amount of chemicals while maintaining yield. Zhang *et al.* prepared a near infrared light-response and magnetic imidacloprid delivery system by introduction of CuS–polydopamine and ferriferous oxide into agarose hydrogel.[4] The nanoplatform could control release of pesticides, and could be reutilized by magnetic collection, which decreased pesticide usage and environmental pollution. With the development of these applications, the quantity of nanoparticles discharged into the environment gradually increased. Nanomaterials could interact with soil, microorganisms and plants, accumulate in plant tissues, and affect the

[a] *Department of Materials Science and Engineering, Jinan University, Guangzhou 511443, China. E-mail: liumx@jnu.edu.cn*
[b] *Biotechnological Institute of Chinese Materia Medica, Jinan University, Guangzhou 510632, China. E-mail: tzhujh@jnu.edu.cn*

† Electronic supplementary information (ESI) available. See DOI: 10.1039/d1en00507c

‡ These authors contributed equally to this work.

growth of plants. This further poses a potential threat to human health through the food chain.[5] Therefore, it is ultimately important to understand the response of plants to nanoparticle exposure, which can open up a new frontier in crop production and food safety.

An increasing number of studies have focused on the toxic effects of nanomaterials on plants by measuring the germination rate, biomass accumulation, plant cell viability, and active oxygen content. Khodakovskaya *et al.* found that multiwalled carbon nanotubes (CNTs) could penetrate tomato seeds, which affected the germination and growth rate of the seeds but increased the biomass of tomatoes.[6] CNTs also had a positive effect on the seed germination of other crops such as wheat, corn, peanuts, and garlic.[7,8] When the concentration of CNTs was low, it was beneficial to plant growth, but it was harmful when the concentration was high. It was found that CNTs with high concentrations (800 μg mL^{-1}) inhibited seed germination and seedling growth, increased cell damage index, and changed antioxidant enzyme activity.[9] The high concentration of nanotubes adsorbed on the plant root surface clogged the pores on roots and root hairs, so they hindered the absorption of water and nutrients, which consequently inhibited the growth and development of plants.[10] Lin *et al.* also found that CNT aggregates reduced the chlorophyll content of Arabidopsis cells.[11] Similarly, a low concentration of SiO_2 nanoparticles increased the germination rate of tomato and corn seeds,[12] while a high concentration of SiO_2 (2 mM) reduced resistance and membrane integrity, increased lipid peroxidation of soybean seedlings, and reduced soybean biomass.[13] When the concentration of fullerene C_{60} was 100 mmg mL^{-1}, it inhibited the root and stem length of *Arabidopsis thaliana*.[14] De La Torre-Roche *et al.* found that when the concentration of fullerene was 500–5000 mg kg^{-1}, it reduced the biomass and net growth of corn and soybean.[15] Zhao *et al.* found that water-soluble fullerene C_{60} was a free radical scavenger, which caused excessive production of active oxygen in the chloroplast of cucumber.[16] In addition, CuO and ZnO nanoparticles significantly reduced the wheat root length and leaf chlorophyll content, and increased root lipid peroxidation.[17] However, another research found that ZnO nanoparticles increased the biomass and photosynthesis of wheat, promoted gas exchange and inhibited oxidative stress.[18] The different effects of nanoparticles on plants may come from the difference in the particle size, morphology, surface properties, and impurity content of nanoparticles.

Halloysites nanotubes (HNTs), whose chemical formula is $Al_2Si_2O_5(OH)_4{\cdot}nH_2O$, are natural one-dimensional clay with a high aspect ratio and a hollow lumen structure. The inner diameter, outer diameter, and length of HNTs range 10–30 nm, 30–50 nm, and 100–2000 nm, respectively.[19] The external surfaces of HNTs are mainly composed of silicon–oxygen (Si–O) groups with a negative charge, and the inner surfaces consist of aluminoxane (Al–OH) groups with a positive charge.[20] HNTs have good biocompatibility and high absorption ability towards drugs, so they are often used as drug delivery carriers,[21] biomaterials for tissue engineering,[22] waste adsorbents, *etc.*[23] HNTs are capable of improving the mechanical properties, cell affinities, drug loading ability of biomaterials. The *in vitro* and *in vivo* toxicity of HNTs towards different cells and animals had also been widely reported,[24] and it had been confirmed that HNTs have high biosafety. In *in vivo* experiments, HNTs after being ingested by nematodes were localized exclusively within the intestines and did not induce any toxic effects.[25] Moreover, it was found that HNTs loaded with curcumin or permethrin suppress the overgrowth of pathogenic bacteria in *Caenorhabditis elegans* nematodes.[26,27] Recently, HNTs have been used as carriers of pesticides and fertilizers.[28,29] Since HNTs have many outstanding advantages, they have promising potential in controlling the loss of pesticides and fertilizers in agriculture. HNTs in the environment may display high bioavailability, thus their potential toxicity urgently needs to be completely assessed. Understanding how plants respond to HNT exposure is an important issue and may open up new areas for crop production and agriculture. With the advance of industrial products based on HNTs and agrochemicals carriers, it is urgent to study their phytotoxicity. But there are few reports on the influence of raw HNTs on plant seed germination and growth as well as cytotoxicity in plant systems.

In this work, the phytotoxicity of raw HNTs was studied using wheat as a plant model and tobacco cells as a cell model. The germination rate and plant growth of the wheat treated with HNTs were recorded. The influence of HNTs on the biomass (including root length, shoot length, fresh weight), chlorophyll content, and oxidative damage index was investigated in detail. The results showed that HNTs can promote growth of wheat at low concentration (0.1–10 mg mL^{-1}) and depress the growth at high concentration (100 mg mL^{-1}). The promotion of plant growth is related to the supplementation of the silicon element by HNTs, while the inhibition of plant growth is due to the clogging of the pore structure by a high-concentration of HNTs. HNTs at high concentration can slightly decrease the viability of tobacco cells but promote the accumulation of biomass and secondary metabolites. This research improved understanding of the interactions between HNTs and plants, which promotes the application and development of HNTs in the agriculture and environmental protection field.

2. Experimental

2.1 HNT dispersion preparation and seed pre-treatments

HNTs were purchased from Guangzhou Runwo Materials Technology Co., Ltd., China. Ultrapure water was prepared from a Milli-Q Integral Water Purification System. An HNT dispersion of 0.1, 1, 10, 100 mg mL^{-1} was obtained by ultrasonication for 30 min. The morphology of HNTs was characterized by using transmission electron microscopy (TEM) (JEM-1400F, JEOL Ltd., Japan), field emission-scanning electron microscopy (Zeiss Sigma 500, Germany), and atomic force microscopy (AFM) (Veeco Instrument Inc). Fourier transform infrared (FTIR) spectra of HNTs was obtained with a Thermo

FTIR (NicoletiS50, Thermo Fisher Scientific Co. Ltd., USA) spectrometer, and X-ray diffraction (XRD) patterns was determined by using XRD instrument (Rigaku, Miniflex600, CuKα, Japan). The zeta potential and particle size distribution of HNTs dispersion were measured by a Zetasizer Nano ZS (Malvern Instruments Co., U.K.). Wheats seeds were obtained from the Institute of Crops, Shandong Academy of Agricultural Sciences, China. Hand-selected seeds of uniform size were rinsed three times with deionized water. Next, the seeds were presoaked in deionized water or the same volumes of 0.1, 1, 10, and 100 mg mL^{-1} HNT dispersion for 8 h. The used HNT concentrations were based on a previous study.[24] Then, the soaked seeds were placed on filter paper moistened with 4 mL deionized water (control) or the same volumes of 0.1, 1, 10, and 100 mg mL^{-1} HNT dispersion in glass Petri dishes of 90 mm diameter. Ten seeds per Petri dish (with ~1 cm distance between each seed) were used for each treatment. The Petri dishes were placed in a culture room at 25 °C with a relative humidity of 70%. The samples were irradiated under 16 h light and 8 h dark photoperiods for 1 week, and they were moistened with the same volumes of deionized water or HNT dispersion to avoid drying.

2.2 Germination and plant growth

The germination rate of wheat seeds exposed to HNT dispersion is tested as follows. The seeds were presoaked in deionized water or the same volumes of 0.1, 1, 10, and 100 mg mL^{-1} HNT dispersion for 8 h. Then, the soaked seeds were placed on filter paper moistened with 4 mL deionized water (control) or the same volumes of HNT dispersion (0.1, 1, 10, and 100 mg mL^{-1}) in glass Petri dishes of 90 mm diameter. Seed germination rate was recorded at 3 days and 7 days. When the radicle broke through the seed coat by 2 mm, the seeds were considered to have germinated.

The germination percentage (GP) was calculated using the following formula:[30]

$$\mathrm{GP} = \frac{n}{N} \times 100\%$$

where GP is the final germination percentage (%); n is the number of germinated seeds; and N represents the total number of seeds in the experiment.

The root and shoot length were measured using a ruler (ten for each group). The 7 day-old wheat plants were washed with deionized water, then the surface was dried and weighed to obtain fresh weight. The sections of the root tip about 3 cm from the end and leaf at half height were observed and photographed with an optical microscope (OLYMPUS BX51, Japan), and then the thickness of the root was measured with ImageJ to obtain the root diameter and leaf width.

2.3 Chlorophyll content

After cultivating the wheat seeds for 7 days, fresh leaves (0.15 g) of the control sample or HNT treated groups were macerated in a mortar, and a small amount of quartz sand, calcium carbonate and 95% ethanol was added, ground and filtered. The chlorophyll was measured using a UV-vis spectrophotometer (Cary 5000, Agilent, USA). The absorbance at 665 nm and 649 nm corresponding to chlorophyll *a* and *b* was measured, respectively.[31]

2.4 Uptake and transport of HNTs in wheat roots

The mixture of HNTs and rhodamine B was stirred without light for 24 h to label HNTs. Then, the suspensions were centrifuged and washed repeatedly with deionized water until free rhodamine B was removed completely. Finally, rhodamine B labeled HNTs were obtained by freeze-drying. FITC labeled HNTs were obtained using a similar procedure. To study the uptake and transport of HNTs, wheats were incubated with the fluorescence labeled HNTs for 24 h. After incubation, the wheat roots were observed using an inverted fluorescence microscope (Zeiss Vert.A1, Germany).

2.5 Determination of ion contents in roots

Ions were extracted from 0.02 g wheat root with a nitric acid and hydrogen peroxide (30% w/v aqueous solution) mixture (volume ratio: 3 : 2) at 80 °C for 3 h and then 160 °C for 5 h. The concentration of Al, Si, Zn, Fe, Mn, and Cu in the obtained extracts was measured using ICP-MS (Agilent 7700, USA).[32]

2.6 Lipid peroxidation analysis, hydrogen peroxide (H_2O_2) and malondialdehyde (MDA) measurement

The cell membrane permeability of the seedlings was evaluated using the electrolyte leakage index (ELI).[33] Leaves (0.1 g) were rinsed with deionized water, then placed in deionized water at 25 °C for 24 h, and the first electrical conductivity of the solution (EC_1) was recorded using a conductivity meter (Leinuo DDS-11A, China). Next, the sample was boiled at 100 °C for 0.5 hours and the second conductivity (EC_2) was recorded subsequently after cooling to 25 °C. The ELI is calculated as follows:

$$\mathrm{ELI}\ (\%) = \frac{\mathrm{EC}_1}{\mathrm{EC}_2} \times 100\%$$

The H_2O_2 content was measured by the method described by Patterson *et al.* with some modifications.[34] Fresh leaves (0.1 g) were homogenized in 1 mL of cold acetone and centrifuged at 8000 × *g* for 5 min at 4 °C. Then, amounts of 0.25 mL of 5% $Ti(SO_4)_2$ and 0.5 mL of NH_4OH were added to the supernatant, and the mixture was centrifuged at 4000 × *g* for 5 min. The obtained precipitate was dissolved in 0.25 mL of 2 M H_2SO_4, and the absorbance was measured at 415 nm using a microplate reader (Cytation 3, BioTek, USA). The H_2O_2 contents were calculated using a standard calibration curve constructed using known concentrations of H_2O_2 and expressed as μmol g^{-1} fr. wt.

The level of lipid peroxidation was measured in terms of the malondialdehyde (MDA, a product of peroxidation of lipids) content by a thiobarbituric acid (TBA) reaction.[35] Fresh leaves (0.1 g) were homogenized in 1 mL of 5%

trichloroacetic acid (TCA) and centrifuged at 4000 × *g* for 10 min. 1 mL of 20% (w/v) TCA containing 0.5% (w/v) thiobarbituric acid (TBA) was supplemented in 50 μL of supernatant aliquot. The mixture was heated in a water bath at 95 °C for 30 min and then cooled with running water. Then the absorbance of the supernatant at 532 nm was recorded. And the MDA content was computed and expressed as nmol g^{-1} fr. wt.

2.7 Scanning electron microscopy (SEM)

Wheat seeds were cultured for 7 days in deionized water (control) or the same volumes of 0.1, 1, 10, and 100 mg mL^{-1} HNT dispersion. The fresh wheat roots were washed with deionized water and put in a fixative composed of 2% glutaraldehyde and 0.05 M phosphate buffer (pH 7.2) for 48 hours. Samples were rinsed with distilled water, dehydrated with an ethanol series (25%, 50%, 75%, 95% and 100%), and replaced with *tert*-butanol. Then, the samples were freeze-dried and cut out to obtain the cross sections. The sections were examined by SEM at 5 kV (Zeiss Sigma 500, Germany). Energy dispersive spectrometer (EDS) mapping was conducted on Si and Al element.

2.8 Effect of HNTs on tobacco cells

The methods to investigate the effect of HNTs on tobacco cells, including cell viability, phenylalanine ammonia lyase, total phenols, catalase activity, and glucose-6-phosphate dehydrogenase, the biomass of tobacco cells and the effect of HNTs on the pH of the culture medium are described in detail in ESI† experiments S1–S8.

3. Results and discussion

3.1 Characterization of the raw HNTs

The phytotoxicity of nanoparticles depends on the type, concentration, particle size, and charge properties of nanoparticles.[36] Before conducting the phytotoxicity measurement, the structure and the morphology of HNTs were determined. The TEM and SEM images of HNTs are shown in Fig. 1A and B. HNTs show typical tubular structures with a hollow lumen and obviously sharp and smooth walls. The diameter of HNTs ranges from 50 to 70 nm and the length of the tubes is in 200–1000 nm. HNTs also possess a smooth and regular tube morphology as seen from the AFM images (Fig. 1C). As shown in Fig. 1D, the diffraction peaks of HNTs appear at 12°, 20°, and 25°, which are attributed to the (001), (020, 110), and (002) planes, respectively.[37] HNTs show characteristic absorption peaks at 3695 and 3623 cm^{-1}, which are ascribed to the O–H stretching of inner-surface hydroxyl groups and inner hydroxyl groups, respectively.[38] Fig. 1F shows that HNTs have a narrow particle size distribution with an average size of 249.3 nm. The zeta potential of HNTs is −33.2 mV, indicating that HNTs have good dispersion stability in water. The uniform tubular morphology and high purity of the raw HNT materials ensure the reliability and repeatability of the following biological data. The cuticle of the root periderm is the first barrier for nanoparticle uptake in plants. The negatively charged nanoparticles were uptaken into the root

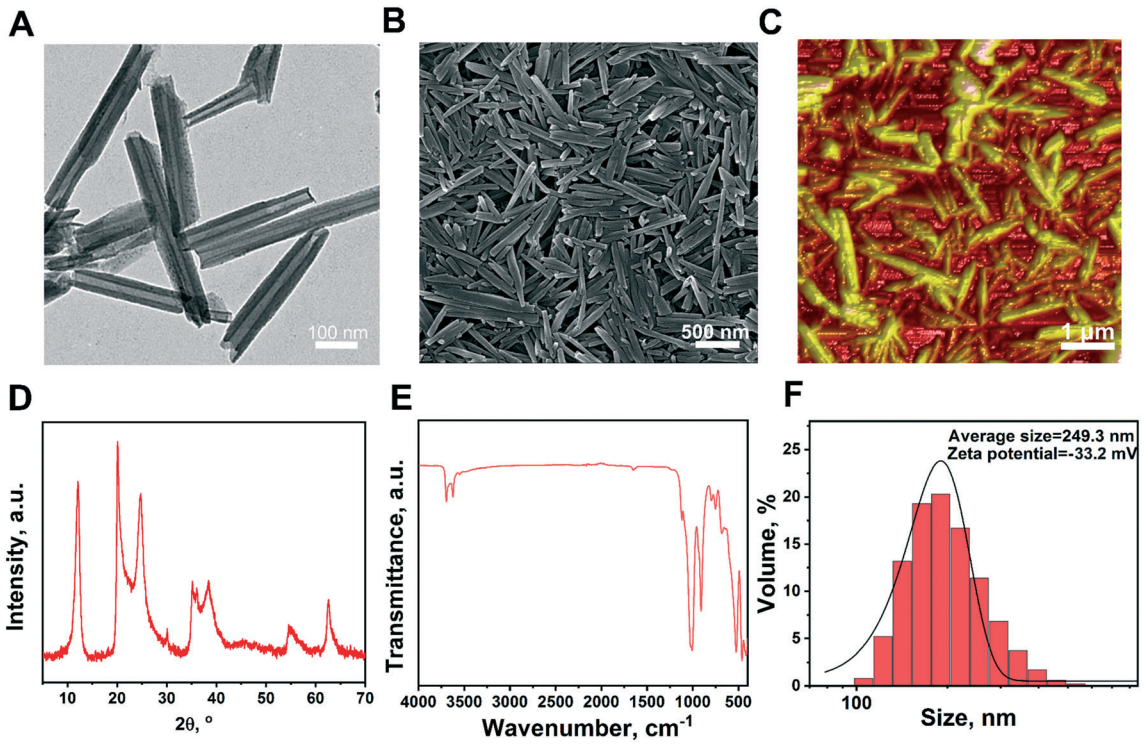

Fig. 1 (A) TEM, (B) SEM, and (C) AFM images, (D) XRD, (E) FTIR, and (F) particle size distribution and zeta potential of the HNTs.

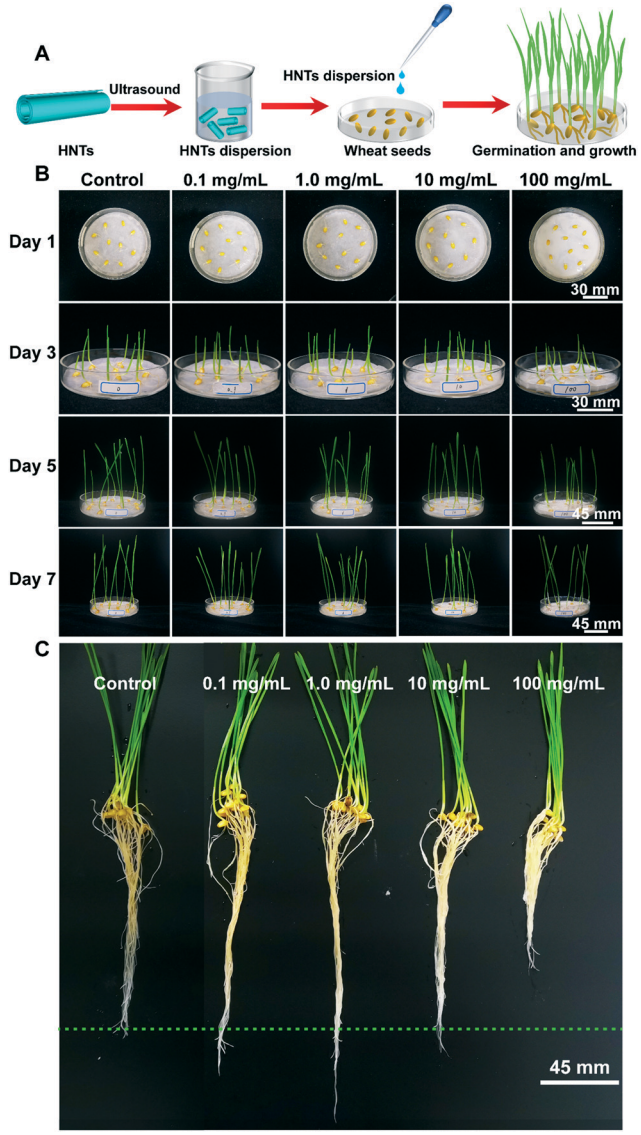

Fig. 2 (A) The schematic diagram of the wheat cultivation process, the photos of (B) wheats cultured in HNT dispersion of different concentrations for 1, 3, 5, and 7 days and (C) wheat seedlings after culturing for 7 days.

system through the cuticle, for example, the negatively charged silica nanoparticles (200 nm) were uptaken into the root system of *A. thaliana*.[32] The negatively charge HNTs display high bioavailability in the environment, which would increase the possibility of their entry into plant roots.

3.2 Effect of HNTs on wheat germination and growth

To test whether HNTs can affect the germination and growth of plants, wheat seeds were placed in petri dishes containing HNT dispersion of different concentrations or deionized water as a control (Fig. 2A). Since the seed absorbs water from its environment during gemination, when the radicle appears, the seed coat ruptures, exposing the plant directly to the test solution. In order to correctly study the germination rate of different groups, the seeds should be exposed to the test solution during the entire elongation period (preferably ≥4 d). The gemination and growth experiments of wheat conducted on filter papers were commonly used.[7,9] From Fig. 2B, compared with the control group, HNTs have no obvious effect on the germination and total height of wheat at different culture times. Wheat seeds germinate and grow well in all the groups, even at a high HNT concentration group. However, HNTs have a significant effect on the roots as observed from Fig. 2C. Small amounts of HNTs promote the growth of roots, while high concentrations of HNTs (100 mg mL^{-1}) inhibit it. When HNTs were used as carriers for pesticides and fertilizers, the content of HNTs in the soil will increase. Nanoparticles could turn into sediments *via* aggregation and settling owing to other factors of soil, such as pH, calcium ion concentration, and the presence of other types of natural colloids.[39] Numerous studies have shown that beyond a certain concentration, nanoparticles will produce toxic effects. HNTs will still affect the growth of wheat when they reach a certain concentration. But, HNTs do not affect the germination rate of wheat. The germination rates of wheat cultured with HNTs are similar to those of wheat without HNTs. Other nanotubes such as CNTs would also not inhibit the germination of wheat seeds.[7] Subsequently, the roots, height and chlorophyll of wheat seedlings were measured in detail.

The germination rate assay is a simple and effective method to evaluate the HNT phytotoxicity to crops, and has been widely used to understand the interactions between different nanomaterials and plants.[6,7,12] As shown in Fig. 3A, the germination rate of wheat seeds containing HNTs is not significantly different from that of the control group, since the GP is close to 100% for all the groups. This suggests that HNTs are environmentally-friendly and have no significant effect on the germination of wheat seeds even at a high dose of 100 mg mL^{-1}. The high biosafety of HNTs has been widely recognized in recent years.[24,25,40] The biomass at 3, 5, and 7 days was then measured to study the influence of HNTs on the growth of wheat seedlings. As can be seen from Fig. 3B and D, the biomass of wheat seedlings germinated and developed on petri dishes at low HNT concentrations (0.1, 1, and 10 mg mL^{-1}) increased, and the biomass with a high concentration of HNTs (100 mg mL^{-1}) decreased significantly compared with the control group. The root length at 7 days of the seedlings in petri dishes containing HNTs (0.1, 1, and 10 mg mL^{-1}) is 1.2, 1.35, and 1.05 times that of the seedlings in the control group, while the seedlings with a high concentration of HNTs (100 mg mL^{-1}) decreased by 56.4% compared with the control group. This suggests that high concentrations of HNTs depress the root growth by filling the pores at the root surfaces. As far as the length of the shoot is concerned, low concentrations of HNTs also have a positive effect on promoting shoot growth. The high concentration of HNTs depressed the shoot growth on the 3rd and 5th day, while the length of the shoot in the high concentration HNT group on the 7th day was equivalent to that in the control

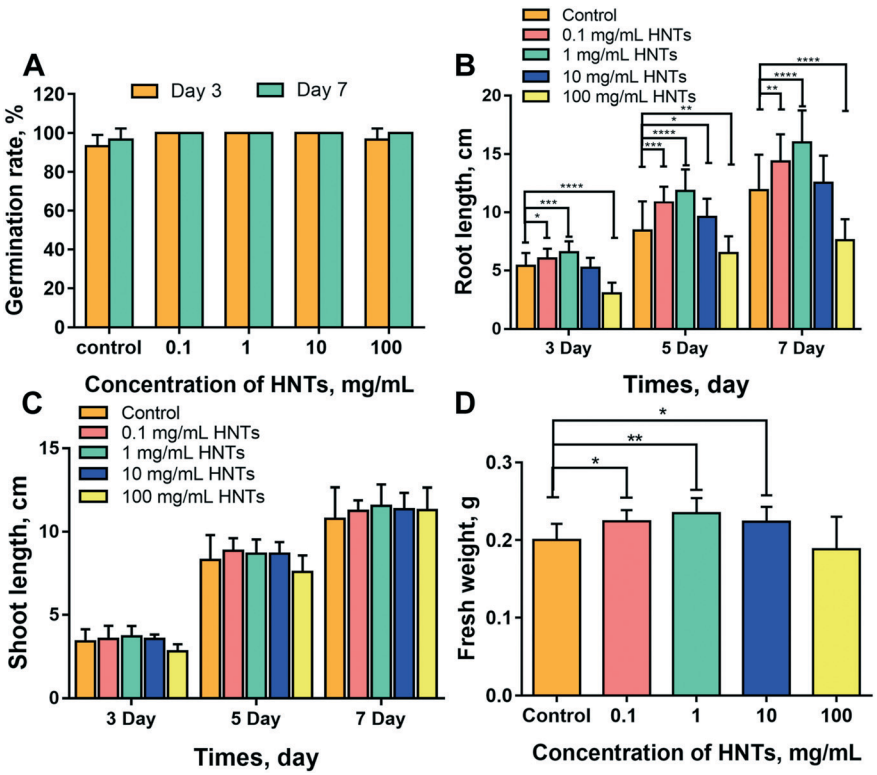

Fig. 3 (A) Germination rate of wheat cultured in HNT dispersion for 3 and 7 days, (B) the root length of wheats and (C) the shoot length of wheats cultured for 3, 5, and 7 days and (D) fresh weight of wheats cultured for 7 days. ****$P < 0.0001$, ***$P < 0.001$, **$P < 0.01$, and *$P < 0.05$ for comparisons of 0.1, 1, 10, and 100 mg mL^{-1} HNTs *versus* control. Error bars show mean ± s.d. (n = 5).

group. The fresh weight of the wheat seedlings at 7 days containing HNTs (1 mg mL^{-1}) increases by 17.4% compared to that of seedlings grown in the control group, but that of the seedlings with a high concentration of HNTs (100 mg mL^{-1}) decreases by 6.5% compared with the control group. From these results, it can be found that the concentration of HNTs affects the germination and growth of wheat. At a relative low dose of the HNTs (below 10 mg mL^{-1}), no symptoms of toxicological effects are observed in the wheat plants. HNTs might promote the root elongation of wheat seedlings by transporting nutrients to the root system. It was reported that other types of nanotubes such as CNTs can also promote root elongation.[7,8]

3.3 Effect of HNTs on root development and leaf size

The root diameter and leaf width of seedlings were further studied to verify the influence of HNTs. Nanoparticles can be deposited on the surfaces of plant root tips, which will reduce the ability of the root system to absorb water and

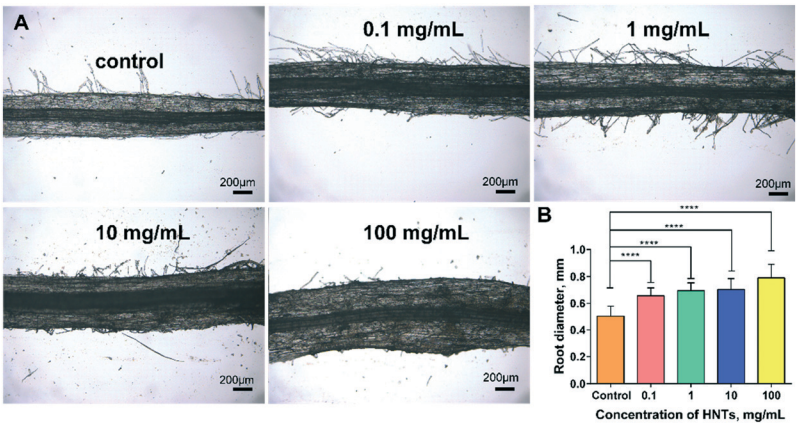

Fig. 4 (A) Optical microscopy photos of wheat roots cultured for 7 days and (B) the root diameter of wheats. ****$P < 0.0001$, ***$P < 0.001$, **$P < 0.01$, and *$P < 0.05$ for comparisons of 0.1, 1, 10, and 100 mg mL^{-1} HNTs *versus* control. Error bars show mean ± s.d. (n = 5).

nutrients. The influence of HNTs on the root morphology was then investigated. As shown in Fig. 4A and B, the root diameter of wheat seedlings cultured with different concentrations of HNTs (0.1, 1, 10, and 100 mg mL^{-1}) increases by 30%, 38%, 40%, and 56.8% respectively compared with the control group. It is considered that root hair proliferation is an adaptive response to nanoparticle deposition. Root hairs can increase the absorption area of the root system. Root hair is the polarization product of root epidermal cells, and its initiation and growth (elongation) are regulated by different genomes, and it is sensitive to hormone substances. Upon adding HNTs to the culture medium, the growth environment becomes water deficient and dry. Due to the adaptive response of the wheat, the length and diameter of HNT treated wheat groups increase. Also, the root hairs of the HNT treated groups are more than those of the control group (data not shown). In fact, other nanoparticles such as TiO_2 and CuO nanoparticles are also able to stimulate the formation of root hair.[41,42] In Fig. 5, the half-leaf width of wheat cultivated with different concentrations of HNTs on the 7th day also slightly increases compared with the control group. The increase in leaf size is beneficial for the development of photosynthesis room. All these results demonstrate that HNTs can promote wheat growth at a certain concentration and show slight phytotoxicity at a relative concentration.

3.4 Effect of HNTs on the chlorophyll content and oxidative damage index

Phenotypic observations of roots, shoots and seed germination were used to investigate the phytotoxicity of HNTs. In the present study, the GP along with root and shoot lengths and fresh weight was positively affected by the lower concentrations of HNTs, however, higher doses inhibited seedling growth. As we know, the chlorophyll content and oxidative damage are two critical indices of plant growth. Chlorophyll absorbs energy from sunlight, which is used by plants to produce organic matter, and plays an important role in making plants green and healthy. Chlorophyll *a* is the main photosynthetic pigment and chlorophyll *b* is a ubiquitous auxiliary pigment in plants. The ratio of the chlorophyll *a*/*b* content controls the absorbed light intensity.[43] Since chlorophyll is extremely important for metabolic processes, an increase in chlorophyll content or an increase in chlorophyll *a*/*b* content ratio may bring problems for plants. HNTs can enter the plant *via* the uptake process during water transportation, and affect the plant growth and the chlorophyll synthesis. As shown in Fig. 6A, the chlorophyll content of wheat seedlings in the HNT-treated groups increases. For example, the chlorophyll content of the 1 mg mL^{-1} HNT group is 13%, which is higher than that of the seedlings in the control group. In Fig. 6B, at a certain concentration of HNTs, the ratio of chlorophyll *a*/*b* in seedlings cultured with HNTs is slightly lower than that of the control group. However, in the case of high-concentration HNTs, the ratio of chlorophyll *a*/*b* is higher than that of the control group. The ratio of the chlorophyll *a*/*b* content controls the intensity of absorption light. At a higher content ratio, plants show an adaptive response, which prevents the chloroplast from maximizing the light-collecting ability, thereby the photosynthetic electron transport capacity is changed.[44] Therefore, high concentrations of HNTs may inhibit the light absorption, photosynthetic electron transfer ability and photosynthesis process of plants, and these nanotubes may affect the transportation of water and nutrients from roots to leaves of plants, thus affecting their photosynthesis.

The phytotoxicity of HNTs towards plants may arise from oxidative stress. A series of oxidative damage indices (cell membrane permeability, H_2O_2 content, MDA content) were determined. As shown in Fig. 6C and D, the ELI and H_2O_2 contents of wheat seedlings at lower concentrations of HNTs are lower than those of the control group, while the indices of seedlings at high concentrations of HNTs (100 mg mL^{-1}) are higher than those of the control group. Low-dose HNTs reduce the leakage of active oxygen and slightly affect electrolytes in seedlings. MDA is considered as a general index of lipid peroxidation. The seedlings generated from seeds exposed to low doses of HNTs (0.1–1 mg mL^{-1}) show a

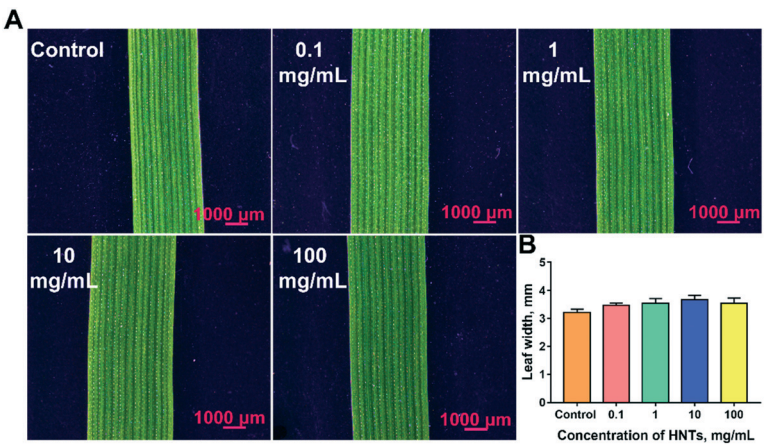

Fig. 5 (A) The stereomicroscope images and (B) the width of wheat leaf cultured in HNT dispersion of different concentrations for 7 days.

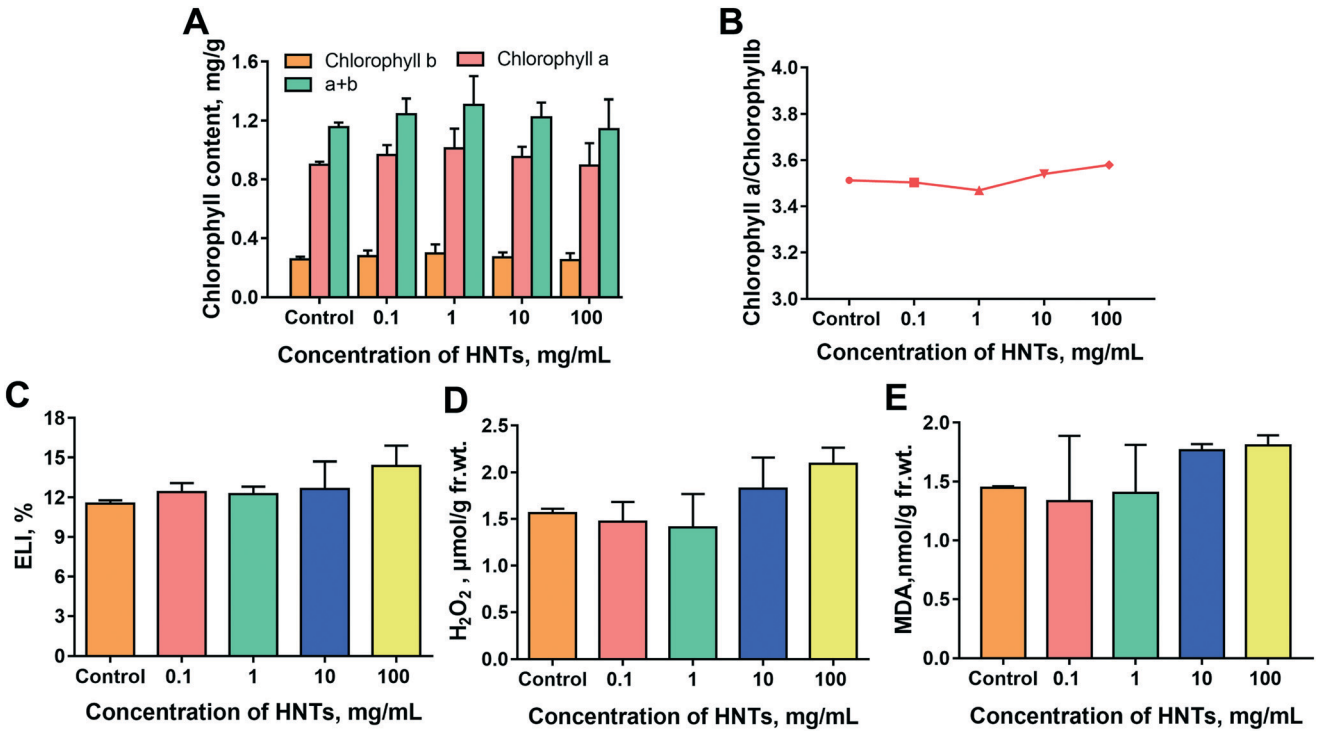

Fig. 6 (A) Chlorophyll content, (B) the ratio of chlorophyll *a* and chlorophyll *b*, (C) electrolyte leakage index (ELI), (D) hydrogen peroxide (H_2O_2), and (E) MDA content of wheat leaves cultured in HNT dispersion at different concentrations for 7 days.

decreased MDA content (Fig. 6E). However, high-dose HNTs increase the MDA content, reactive oxygen species (ROS) and electrolyte leakage, indicating that the stability of the cell membrane is reduced. It is recognized that the structural stability of cell membranes could protect plant tissues from osmotic stress.[45] In addition, the growth of seedlings treated with high-dose HNTs (100 mg mL^{-1}) was observed to be worse than that of the control group, which may be due to excessive production of ROS and MDA. However, although the seedlings treated with 10 mg mL^{-1} HNTs produced higher ROS and MDA than the control group, the growth of the seedlings and the electrolyte leakage index (Fig. 6C) were not much different from those of the control group. This may be because the MDA content produced does not threaten the stability of the cell membrane, so it has no obvious effect on the growth of seedlings. Thus, low-dose HNTs are able to stabilize cell membranes and stimulate wheat growth, while high-dose HNTs reduce cell membrane stability and inhibit wheat growth.

3.5 Uptake and transport of HNTs by wheat roots

HNTs could promote the growth of seedlings, which might be due to the fact that they can penetrate root systems as well as allow water absorption in roots. Nanoparticles of various components and sizes can be absorbed by plants, which changes the germination of roots, leaves and seeds of plants, and may cause genetic changes. The physical and chemical properties of nanoparticles, such as size, crystal structure, and surface charge, will affect their translocation and bioaccumulation in plants. The uptake of nanoparticles by crops can enter the food chain *via* roots or foliar uptake, which brings safety concerns. HNTs can be uptaken by different animal cells, which has been widely reported. But up to now, few evidence of HNTs entering plants has been reported. The images of roots of wheat seedlings incubated in rhodamine B-labeled HNT solutions using a fluorescence microscope are shown in Fig. 7A. The red fluorescence signals with some aggregated regions, which represented the rhodamine B-labeled HNTs, were clearly observed. The red-light intensities increase with the increase of HNT content, suggesting that HNTs can enter the root of the wheat. In order to further confirm the existence of the HNTs in the root, the SEM images of the cross-section of the roots were examined (Fig. 7B). HNTs possess a high aspect ratio and hollow lumen structure, so one could easily identify these tubular particles in SEM images. It can be clearly seen that there are no HNTs in the control group, but HNTs are found in the cortex of roots cultured in HNT dispersion. HNTs in the root are in the aggregated state and the amount of aggregates increases with the increase of HNT loading. The aggregation phenomenon of HNTs in the plant is brought about by the change in ion concentrations, since the plant cells have numerous ions such as K^+ and Na^+. The aggregated HNTs adhere to the pore walls of the plant, and the accumulation of HNTs has negative or positive effects on plant growth. There are also other methods which can also be employed to observe the nanotubes in the plant, such as confocal laser scanning microscopy (CLSM) or dark-field/hyperbranched microscopy.[46]

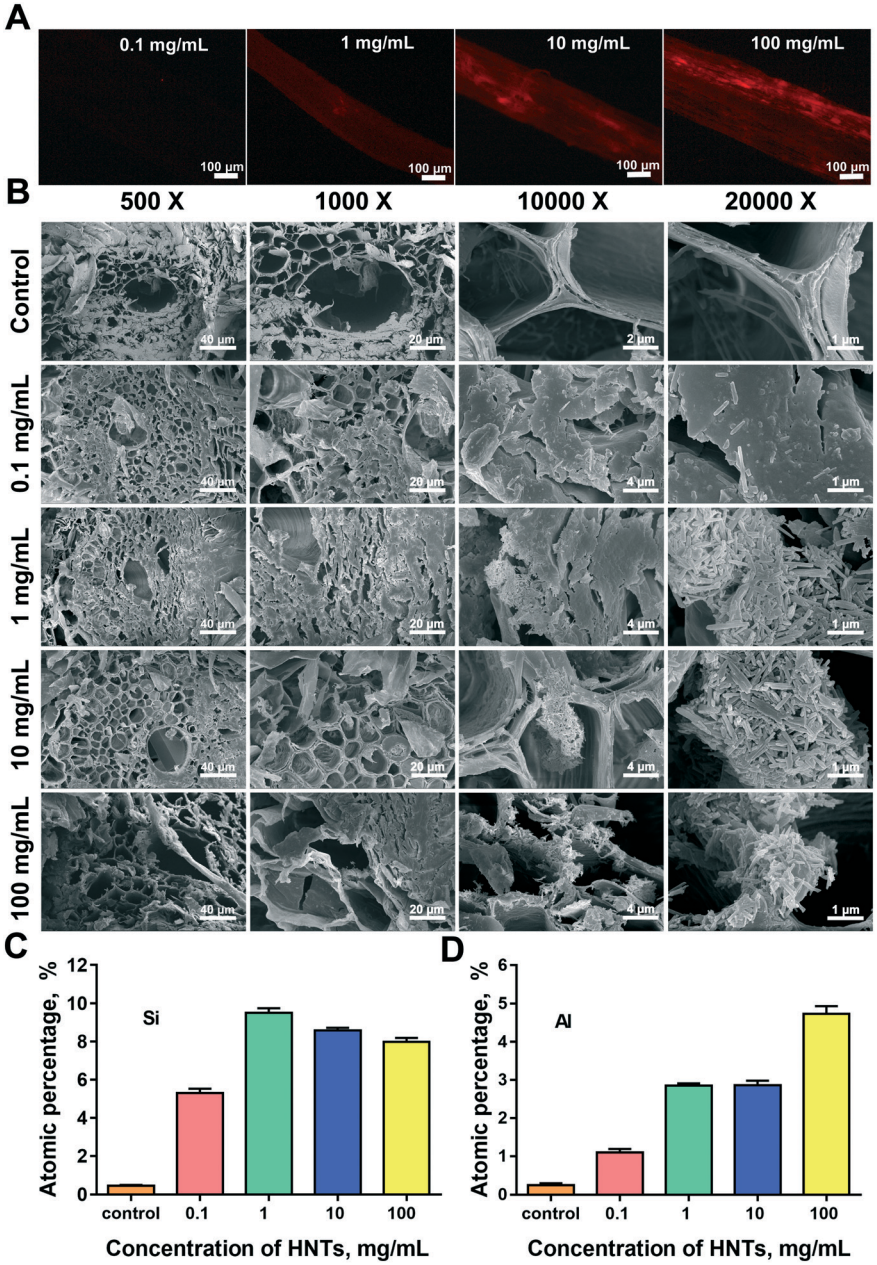

Fig. 7 (A) Fluorescence microscope images of wheat roots cultured with different concentrations of rhodamine B labeled HNTs for 3 days, and (B) SEM images and (C) silicon and (D) aluminum atomic percentage determined by EDS of wheat roots cultured in HNT dispersion of different concentrations for 7 days.

The chemical composition of HNTs contains silicon, which is a beneficial element for plant growth, such as improving tolerance to drought and heavy metals, and improving the quality and yield of crops.[47] It is possible that the biomass of wheat seedlings in HNTs treated groups increases due to the introduction of the silicon element by HNTs. With the increase of the concentration of the HNT dispersion, the amount of HNTs entering the roots also increases (Fig. 7C). For the group of wheat treated with a high concentration of HNTs, the large accumulation of the nanotubes on the root surface may hinder the water transport and water utilization efficiency of the root system, thus reducing transpiration and affecting the growth and development of plants.[48] No HNTs were observed in the xylem in all samples. Generally, the plant root cap is protected by the mucus layer of the boundary cell, which is composed of negatively charged root secretions.[49] There are negatively charged Si–O–Si groups on the outer surface of HNTs, so HNTs will not absorb the mucus at the root boundary, but can enter the root interior. Aluminum contents in the wheat root also increase with the increase of the HNT concentration as shown in Fig. 7D, and aluminum is generally considered detrimental to plant growth. A high content of Al may cause Al phytotoxicity to plants, so one must pay attention to the HNT concentration when using

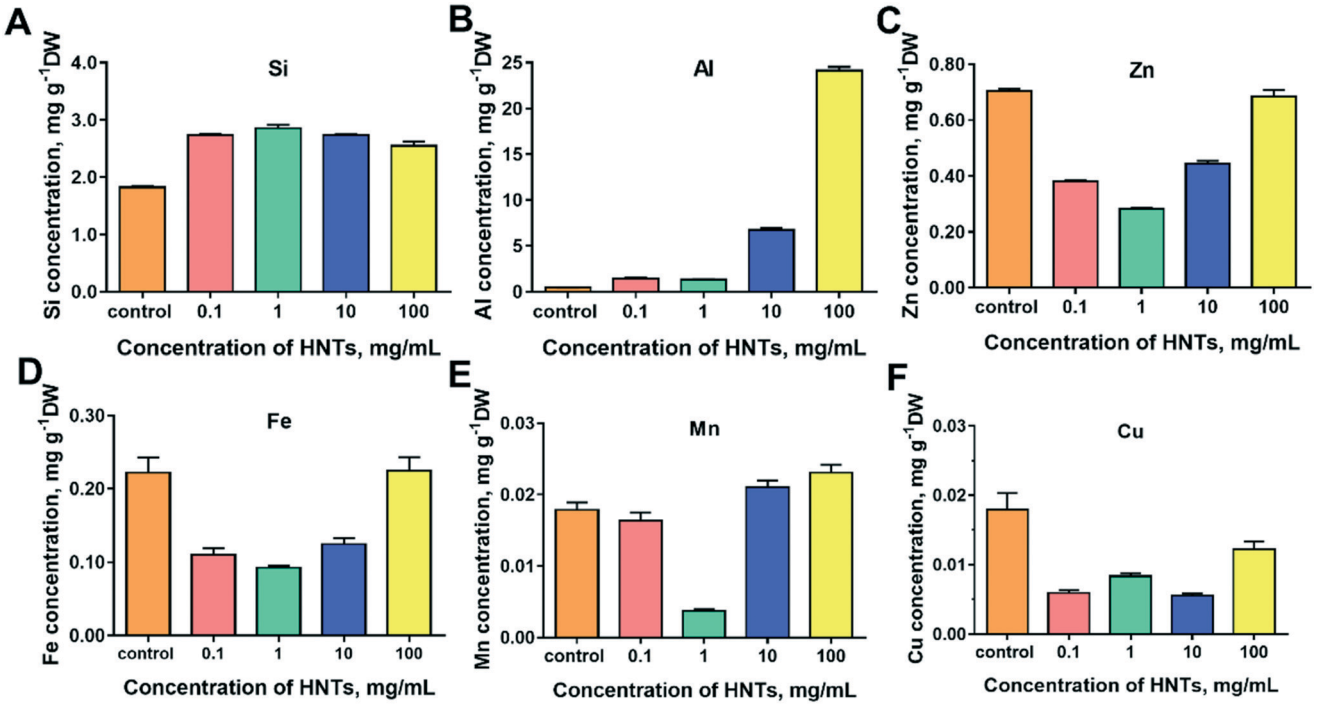

Fig. 8 Si (A), Al (B), Zn (C), Fe (D), Mn (E), and Cu (F) concentrations in roots of wheat plants cultured with different concentrations of HNT dispersion for 7 days.

HNTs as carriers for pesticides or fungicides. These results also show the decrease of the root length and fresh weight of the seedings in the high HNT concentration group. So, the influence of HNTs on wheat growth exhibits a comprehensive result as illustrated above.

Since HNTs are chemically composed of Si, Al and O, the uptake of the tubes in plants can also be measured using ICP-MS. The contents of Si and Al as well as other micronutrient contents (Zn, Fe, Mn, Cu) in root are shown in Fig. 8. The change in the trend of Si and Al contents was consistent with EDS mapping results (Fig. 7C and D). Oxidative stress is a hallmark feature of abiotic stress, and Si can prevent or mitigate the strains imposed by stress.[50] The micronutrient elements (Zn, Fe, Mn, Cu) are necessary for plant growth but should be kept to a very low amount for plants. Otherwise, a high concentration would lead to toxicity for plant life and ultimately death of plants. The Zn, Fe, Mn, Cu concentrations of wheat roots with low-dose HNTs (0.1, 1 mg mL^{-1}) were decreased while those in the high HNT dose groups (10, 100 mg mL^{-1}) were close to those of the control group. This trend is contrary to the root length and fresh weight results in different groups shown in Fig. 2 and 3. This can be understood by the fact that since the Zn, Fe, Mn, Cu elements exist in the wheat seeds but not in HNTs, the bigger root length and weight group (1 mg mL^{-1}) corresponds to the low element content (we used the same weight wheat root for each group). In addition, it was reported that adding Si reduced Zn concentration in maize[51] and alleviated Mn toxicity in cucumber,[52] which significantly increased plant growth and chlorophyll content and reduced membrane permeability. At a moderate HNT concentration of 1 mg mL^{-1}, the Si content is maximum which lowered the Zn, Fe, Mn, and Cu content in wheat roots. HNTs are foreign substances for the growth of wheat, and they are also a source of abiotic stress when their concentration is high. Si from HNTs might provide resistance to oxidative stress in seedlings cultivated with high concentrations of HNTs (10 and 100 mg mL^{-1}). This is also the reason that the increase in the Al concentration of wheat root is consistent with the increase in HNT concentration but it is not consistent with the Si, Zn, Fe, Mn concentration.

Generally, nanoparticles have two basic root absorption and transport pathways in higher plants, *i.e.* the apoplast transport pathway and the symbiotic pathway.[53] Since HNTs are not observed in the xylem, the uptake and transport of HNTs in the roots may be the apoplast pathway. In this way, HNTs first penetrate the pores of the cell wall, and then diffuse to the space between the cell wall and the plasma membrane, or pass through the intercellular space without passing through the cell membrane. The plant cell wall is a semipermeable barrier that regulates the transport of substances through pores, and the size of nanoparticles determines whether they can enter plant roots.[54] Slomberg *et al.* found that as the particle size (14, 50, 200 nm) increases, fewer particles were observed in Arabidopsis roots.[32] Wang *et al.* observed that chitosan modified HNTs can enter the roots of wheat.[28] Nevertheless, further investigation should be performed to demonstrate whether HNTs can enter the leaves, flowers, and fruits. These results suggested that HNTs had an influence on photosynthesis and oxidative stress in seedlings during the transport of nutrients to the root/leaf system.

At the cellular level, cells are more sensitive to external substances and react faster. Some reaction signals of nanoparticles can be reflected at the cell level, but not necessarily at the plant level. Therefore, the experiment of plant cell exposure was supplemented, and the results are described in Fig. S1.† HNTs showed toxicity to tobacco cells potentially, and the toxicity was time-and dose-dependent. These results are similar to the effect of HNTs on wheat growth in a dose-dependent manner. HNTs are safe at low concentration and even have a positive effect on the growth of tobacco cells and secondary metabolites. Besides, HNTs stimulate cellular defense responses and respond to environmental pressures through changes in cellular catalase activity. The discussion is described in detail in the ESI.†

4. Conclusion

This work demonstrates that HNTs do not affect the germination of wheat seeds, but they affect the growth of wheat seeds in a dose-dependent manner. The biomass and chlorophyll content of wheat seedlings are higher than the control group when the wheat is exposed to 1 mg mL^{-1} HNT dispersion. A high concentration of HNTs (100 mg mL^{-1}) can depress the biomass and chlorophyll content of wheat. HNTs are capable of entering and accumulating in the wheat roots, which affect water transport at high doses. HNTs (0.1, 1 mg mL^{-1}) reduce the MDA content and H_2O_2 content, while high-dose HNTs increase the MDA content, produce excessive ROS, and improve cell membrane permeability. At the cellular level, the cytotoxicity of HNTs to tobacco cells is time- and dose-dependent. HNTs are safe at low concentration and even have positive effect on the growth of tobacco cells and secondary metabolites. This study will increase the understanding of the phytotoxicity of HNTs and provide possibilities for the development of HNTs for application in the agricultural field.

Conflicts of interest

There are no conflicts to declare.

Acknowledgements

This work was financially supported by the National Natural Science Foundation of China (52073121), the Natural Science Foundation of Guangdong Province, China (2019A1515011509), the Guangdong Province Natural Science Fund for Distinguished Young Scholars, China (2016A030306009), and the Fundamental Research Funds for the Central Universities (21619102).

References

1 R. Prasad, A. Bhattacharyya and Q. D. Nguyen, Nanotechnology in sustainable agriculture: recent developments, challenges, and perspectives, *Front. Microbiol.*, 2017, **8**, 1014.
2 R. C. Choudhary, R. Kumaraswamy, S. Kumari, S. Sharma, A. Pal, R. Raliya, P. Biswas and V. Saharan, Zinc encapsulated chitosan nanoparticle to promote maize crop yield, *Int. J. Biol. Macromol.*, 2019, **127**, 126–135.
3 N. Kottegoda, C. Sandaruwan, G. Priyadarshana, A. Siriwardhana, U. A. Rathnayake, D. M. Berugoda Arachchige, A. R. Kumarasinghe, D. Dahanayake, V. Karunaratne and G. A. Amaratunga, Urea-hydroxyapatite nanohybrids for slow release of nitrogen, *ACS Nano*, 2017, **11**, 1214–1221.
4 L. Zhang, S. Ren, C. Chen, D. Wang, B. Liu, D. Cai and Z. Wu, Near infrared light-driven release of pesticide with magnetic collectability using gel-based nanocomposite, *Chem. Eng. J.*, 2021, **411**, 127881.
5 M. Rui, C. Ma, Y. Hao, J. Guo, Y. Rui, X. Tang, Q. Zhao, X. Fan, Z. Zhang and T. Hou, Iron oxide nanoparticles as a potential iron fertilizer for peanut (Arachis hypogaea), *Front. Plant Sci.*, 2016, **7**, 815.
6 M. Khodakovskaya, E. Dervishi, M. Mahmood, Y. Xu, Z. Li, F. Watanabe and A. S. Biris, Carbon nanotubes are able to penetrate plant seed coat and dramatically affect seed germination and plant growth, *ACS Nano*, 2009, **3**, 3221–3227.
7 A. Joshi, S. Kaur, K. Dharamvir, H. Nayyar and G. Verma, Multi-walled carbon nanotubes applied through seed-priming influence early germination, root hair, growth and yield of bread wheat (Triticum aestivum L.), *J. Sci. Food Agric.*, 2018, **98**, 3148–3160.
8 A. Srivastava and D. Rao, Enhancement of seed germination and plant growth of wheat, maize, peanut and garlic using multiwalled carbon nanotubes, *Eur. Chem. Bull.*, 2014, **3**, 502–504.
9 M. Hatami, J. Hadian and M. Ghorbanpour, Mechanisms underlying toxicity and stimulatory role of single-walled carbon nanotubes in Hyoscyamus niger during drought stress simulated by polyethylene glycol, *J. Hazard. Mater.*, 2017, **324**, 306–320.
10 J. Lv, P. Christie and S. Zhang, Uptake, translocation, and transformation of metal-based nanoparticles in plants: recent advances and methodological challenges, *Environ. Sci.: Nano*, 2019, **6**, 41–59.
11 C. Lin, B. Fugetsu, Y. Su and F. Watari, Studies on toxicity of multi-walled carbon nanotubes on Arabidopsis T87 suspension cells, *J. Hazard. Mater.*, 2009, **170**, 578–583.
12 M. E. El-Naggar, N. R. Abdelsalam, M. M. Fouda, M. I. Mackled, M. A. Al-Jaddadi, H. M. Ali, M. H. Siddiqui and E. E. Kandil, Soil application of nano silica on maize yield and its insecticidal activity against some stored insects after the post-harvest, *Nanomaterials*, 2020, **10**, 739.
13 S. Farhangi-Abriz and S. Torabian, Nano-silicon alters antioxidant activities of soybean seedlings under salt toxicity, *Protoplasma*, 2018, **255**, 953–962.
14 Q. Liu, Y. Zhao, Y. Wan, J. Zheng, X. Zhang, C. Wang, X. Fang and J. Lin, Study of the inhibitory effect of water-soluble fullerenes on plant growth at the cellular level, *ACS Nano*, 2010, **4**, 5743–5748.
15 R. De La Torre-Roche, J. Hawthorne, Y. Deng, B. Xing, W. Cai, L. A. Newman, Q. Wang, X. Ma, H. Hamdi and J. C.

White, Multiwalled carbon nanotubes and C60 fullerenes differentially impact the accumulation of weathered pesticides in four agricultural plants, *Environ. Sci. Technol.*, 2013, **47**, 12539–12547.

16 L. Zhao, H. Zhang, J. Wang, L. Tian, F. Li, S. Liu, J. R. Peralta-Videa, J. L. Gardea-Torresdey, J. C. White and Y. Huang, C60 fullerols enhance copper toxicity and alter the leaf metabolite and protein profile in cucumber, *Environ. Sci. Technol.*, 2019, **53**, 2171–2180.

17 C. O. Dimkpa, J. E. McLean, D. E. Latta, E. Manangón, D. W. Britt, W. P. Johnson, M. I. Boyanov and A. J. Anderson, CuO and ZnO nanoparticles: phytotoxicity, metal speciation, and induction of oxidative stress in sand-grown wheat, *J. Nanopart. Res.*, 2012, **14**, 1–15.

18 M. Rizwan, S. Ali, B. Ali, M. Adrees, M. Arshad, A. Hussain, M. Z. ur Rehman and A. A. Waris, Zinc and iron oxide nanoparticles improved the plant growth and reduced the oxidative stress and cadmium concentration in wheat, *Chemosphere*, 2019, **214**, 269–277.

19 Y. M. Lvov, D. G. Shchukin, H. Mohwald and R. R. Price, Halloysite clay nanotubes for controlled release of protective agents, *ACS Nano*, 2008, **2**, 814–820.

20 E. Joussein, S. Petit, J. Churchman, B. Theng, D. Righi and B. Delvaux, Halloysite clay minerals-a review, *Clay Miner.*, 2005, **40**, 383–426.

21 Y. Lvov, W. Wang, L. Zhang and R. Fakhrullin, Halloysite clay nanotubes for loading and sustained release of functional compounds, *Adv. Mater.*, 2016, **28**, 1227–1250.

22 S. S. Suner, S. Demirci, B. Yetiskin, R. Fakhrullin, E. Naumenko, O. Okay, R. S. Ayyala and N. Sahiner, Cryogel composites based on hyaluronic acid and halloysite nanotubes as scaffold for tissue engineering, *Int. J. Biol. Macromol.*, 2019, **130**, 627–635.

23 L. Yu, H. Wang, Y. Zhang, B. Zhang and J. Liu, Recent advances in halloysite nanotube derived composites for water treatment, *Environ. Sci.: Nano*, 2016, **3**, 28–44.

24 Z. Long, Y.-P. Wu, H.-Y. Gao, J. Zhang, X. Ou, R.-R. He and M. Liu, In vitro and in vivo toxicity evaluation of halloysite nanotubes, *J. Mater. Chem. B*, 2018, **6**, 7204–7216.

25 G. I. Fakhrullina, F. S. Akhatova, Y. M. Lvov and R. F. Fakhrullin, Toxicity of halloysite clay nanotubes in vivo: a Caenorhabditis elegans study, *Environ. Sci.: Nano*, 2015, **2**, 54–59.

26 G. I. Fakhrullina, E. Khakimova, F. Akhatova, G. Lazzara, F. Parisi and R. Fakhrullin, Selective antimicrobial effects of curcumin@halloysite nanoformulation: a Caenorhabditis elegans study, *ACS Appl. Mater. Interfaces*, 2019, **11**, 23050–23064.

27 A. Panchal, G. Fakhrullina, R. Fakhrullin and Y. Lvov, Self-assembly of clay nanotubes on hair surface for medical and cosmetic formulations, *Nanoscale*, 2018, **10**, 18205–18216.

28 C. Wang, Z. He, Y. Liu, C. Zhou, J. Jiao, P. Li, D. Sun, L. Lin and Z. Yang, Chitosan-modified halloysite nanotubes as a controlled-release nanocarrier for nitrogen delivery, *Appl. Clay Sci.*, 2020, **198**, 105802.

29 X. Zeng, B. Zhong, Z. Jia, Q. Zhang, Y. Chen and D. Jia, Halloysite nanotubes as nanocarriers for plant herbicide and its controlled release in biodegradable polymers composite film, *Appl. Clay Sci.*, 2019, **171**, 20–28.

30 I. S. T. Association, International rules for seed testing, *Rules 1999*, 1999.

31 J. Bruinsma, A comment on the spectrophotometric determination of chlorophyll, *Biochim. Biophys. Acta*, 1961, **52**, 576–578.

32 D. L. Slomberg and M. H. Schoenfisch, Silica nanoparticle phytotoxicity to Arabidopsis thaliana, *Environ. Sci. Technol.*, 2012, **46**, 10247–10254.

33 M. Jiang and J. Zhang, Effect of abscisic acid on active oxygen species, antioxidative defence system and oxidative damage in leaves of maize seedlings, *Plant Cell Physiol.*, 2001, **42**, 1265–1273.

34 B. D. Patterson, E. A. MacRae and I. B. Ferguson, Estimation of hydrogen peroxide in plant extracts using titanium (IV), *Anal. Biochem.*, 1984, **139**, 487–492.

35 R. L. Heath and L. Packer, Photoperoxidation in isolated chloroplasts: I. Kinetics and stoichiometry of fatty acid peroxidation, *Arch. Biochem. Biophys.*, 1968, **125**, 189–198.

36 J. Yang, W. Cao and Y. Rui, Interactions between nanoparticles and plants: phytotoxicity and defense mechanisms, *J. Plant Interact.*, 2017, **12**, 158–169.

37 G. Brindley, K. Robinson and D. MacEwan, The clay minerals halloysite and meta-halloysite, *Nature*, 1946, **157**, 225–226.

38 J. Madejová, FTIR techniques in clay mineral studies, *Vib. Spectrosc.*, 2003, **31**, 1–10.

39 J. R. Lead, G. E. Batley, P. J. Alvarez, M. N. Croteau, R. D. Handy, M. J. McLaughlin, J. D. Judy and K. Schirmer, Nanomaterials in the environment: behavior, fate, bioavailability, and effects-an updated review, *Environ. Toxicol. Chem.*, 2018, **37**, 2029–2063.

40 X. Zhao, Q. Wan, X. Fu, X. Meng, X. Ou, R. Zhong, Q. Zhou and M. Liu, Toxicity evaluation of one-dimensional nanoparticles using caenorhabditis elegans: a comparative study of halloysite nanotubes and chitin nanocrystals, *ACS Sustainable Chem. Eng.*, 2019, **7**, 18965–18975.

41 T. Giordani, A. Fabrizi, L. Guidi, L. Natali, G. Giunti, F. Ravasi, A. Cavallini and A. Pardossi, Response of tomato plants exposed to treatment with nanoparticles, *EQA-International Journal of Environmental Quality*, 2012, **8**, 27–38.

42 J. Adams, M. Wright, H. Wagner, J. Valiente, D. Britt and A. Anderson, Cu from dissolution of CuO nanoparticles signals changes in root morphology, *Plant Physiol. Biochem.*, 2017, **110**, 108–117.

43 L. R. R. Souza, L. E. Bernardes, M. F. S. Barbetta and M. A. M. S. da Veiga, Iron oxide nanoparticle phytotoxicity to the aquatic plant Lemna minor: effect on reactive oxygen species (ROS) production and chlorophyll a/chlorophyll b ratio, *Environ. Sci. Pollut. Res.*, 2019, **26**, 24121–24131.

44 M. Dale and D. Causton, Use of the chlorophyll a/b ratio as a bioassay for the light environment of a plant, *Funct. Ecol.*, 1992, 190–196.

45 M. Filek, S. Walas, H. Mrowiec, E. Rudolphy-Skórska, A. Sieprawska and J. Biesaga-Kościelniak, Membrane permeability and micro-and macroelement accumulation in spring wheat cultivars during the short-term effect of salinity-and PEG-induced water stress, *Acta Physiol. Plant.*, 2012, **34**, 985–995.

46 R. Fakhrullin, L. Nigamatzyanova and G. Fakhrullina, Dark-field/hyperspectral microscopy for detecting nanoscale particles in environmental nanotoxicology research, *Sci. Total Environ.*, 2021, 145478.

47 K. E. Richmond and M. Sussman, Got silicon? The non-essential beneficial plant nutrient, *Curr. Opin. Plant Biol.*, 2003, **6**, 268–272.

48 P. Miralles, T. L. Church and A. T. Harris, Toxicity, uptake, and translocation of engineered nanomaterials in vascular plants, *Environ. Sci. Technol.*, 2012, **46**, 9224–9239.

49 A. Avellan, F. Schwab, A. Masion, P. Chaurand, D. Borschneck, V. Vidal, J. R. M. Rose, C. Santaella and C. M. Levard, Nanoparticle uptake in plants: gold nanomaterial localized in roots of Arabidopsis thaliana by X-ray computed nanotomography and hyperspectral imaging, *Environ. Sci. Technol.*, 2017, **51**, 8682–8691.

50 D. Coskun, R. Deshmukh, H. Sonah, J. G. Menzies, O. Reynolds, J. F. Ma, H. J. Kronzucker and R. R. Bélanger, The controversies of silicon's role in plant biology, *New Phytol.*, 2019, **221**, 67–85.

51 C. Kaya, A. L. Tuna, O. Sonmez, F. Ince and D. Higgs, Mitigation effects of silicon on maize plants grown at high zinc, *J. Plant Nutr.*, 2009, **32**, 1788–1798.

52 J. Dragišić Maksimović, J. Bogdanović, V. Maksimović and M. Nikolic, Silicon modulates the metabolism and utilization of phenolic compounds in cucumber (Cucumis sativus L.) grown at excess manganese, *J. Plant Nutr. Soil Sci.*, 2007, **170**, 739–744.

53 F. Schwab, G. Zhai, M. Kern, A. Turner, J. L. Schnoor and M. R. Wiesner, Barriers, pathways and processes for uptake, translocation and accumulation of nanomaterials in plants-Critical review, *Nanotoxicology*, 2016, **10**, 257–278.

54 R. Nair, S. H. Varghese, B. G. Nair, T. Maekawa, Y. Yoshida and D. S. Kumar, Nanoparticulate material delivery to plants, *Plant Sci.*, 2010, **179**, 154–163.

Electronic Supplementary Material (ESI) for Environmental Science: Nano.

Electronic Supplementary Information

Phytotoxicity of halloysite nanotubes using wheat as a model: Seed germination and growth

Linhong Chen[a,†], Zizheng Guo [b,†], Biyin Lao[a], Chunlei Li[b],Jianhua Zhu[b,], Rongmin Yu[b], Mingxian Liu*[,a]*

[a] Department of Materials Science and Engineering, Jinan University, Guangzhou 511443, China

[b]Biotechnological Institute of Chinese Materia Medica, Jinan University, Guangzhou 510632, China

† These authors contributed equally to this work.

* Corresponding author. Email: tzhujh@jnu.edu.cn; liumx@jnu.edu.cn

Supplemental experiment

Experiment S1. Cell suspension cultures

Seeds of tobacco (*Nicotiana tabacum* L.) were purchased from Guangzhou Baihui Biological Technology Co., Ltd, Guangzhou, China. The seeds were immersed in distilled water for 24 h, then immersed in 75% alcohol for 0.5 min and rinsed with sterile water 4 times, additionally immersed in 0.1% (w/v) mercuric chloride solution for 15.0 min followed by four rinses in sterile water. The surface-sterilized seeds were dried by sterile filter paper and implanted on Murashige and Skoog (MS) medium. Plants of tobacco were sub-cultured every 4 weeks. Leaves of tobacco were used as explants to induce callus. Leaves were cut into small pieces about 0.5 cm × 0.5 cm and cultured horizontally on MS solid medium with 1.0 mg L^{-1} α-naphthaleneacetic acid (NAA) and 3.0 mg L^{-1} 6-benzyladenine (6-BA). Callus appeared in 2 weeks. And then, callus was subsequently cut from the explant and further cultured in MS solid medium containing 1.0 mg L^{-1} NAA and 1.0 mg L^{-1} 6-BA. Suspension culture cells of tobacco were obtained by inoculating the callus in MS liquid medium with 1.0 mg L^{-1} NAA and 1.0 mg L^{-1} 6-BA. Unless otherwise stated, all media were contained 30 g L^{-1} sucrose，and 8 g L^{-1} agar for solid media, and adjusted to pH 5.8 before autoclaving at 121^{o}C for 20 min. All plant tissue cultures were maintained at 24 ± 1^{o}C. Plantlets were illuminated with 16/8 (day/night) photoperiod, while the cell were cultured in the dark. Suspension culture cells were cultured in dark with rotating shaking of 100 rpm.

Experiment S2. The cell viability

Suspension culture cells of tobacco were passaged three times before use, once

every 12 days. 20 mL tobacco suspension culture cells (approximately 6 g) were poured into 250 mL Erlenmeyer flask containing 80 mL MS liquid medium with 1.0 mg L^{-1} NAA and 1.0 mg L^{-1} 6-BA. After pre-cultured for 10 d, HNTs was added into the suspension culture cells, and further cultured for another 24, 48 and 72 h, respectively. Cell suspension samples (1 mL) were washed aseptically with 50 mM phosphate buffer (pH 7.5) twice. Then the samples were resuspended in 1 mL of the same buffer.

2,3,5-Triphenyl-2H-tetrazolium chloride (TTC) stock solution, which was freshly prepared by dissolving 0.2 g TTC in 10 mL sterile 50 mM phosphate buffer (pH 7.5), was added to a final concentration of 2.5 mM, and then the samples were incubated for 8 h in the dark at 25°C. Afterwards, formazan salts were solubilized with 50% methanol (containing 1% SDS) at 60°C for a period of 30 min. The sample was centrifuged at 1500 × g for 5 min and the supernatant was recovered. The supernatants were pooled and quantified absorbance at 485 nm using microplate reader.[1, 2]

Experiment S3. Effect of HNTs on the pH of the culture medium

pH value of the culture medium was determined at a serial time interval as 0, 1, 2, 3, 4, 5, 6, 12, 18, 24 h after the addition of HNTs.

Experiment S4. The PAL (phenylalanine ammonia lyase) of tobacco cells

The activity of PAL was determined by measuring trans-cinnamic acid, the catalytic product of PAL.[3] 5 mL suspension culture cells were centrifuged at 1500 × g for 5 min to remove the supernatant, and a small amount of polyvinylpyrrolidone (PVP) was then added. Next, pre-cooled enzyme extract (2 mL containing 5 mmol L^{-1} mercaptoethanol, 1% PVP, 0.1 mol L^{-1} boric acid buffer) and quartz sand were ground

on ice. The grinding solution was transferred to a 5 mL centrifuge tube and centrifuged at 10,000 × g for 15 min to take the supernatant as the crude enzyme extract. 0.02 mol L^{-1} phenylalanine (1 mL) was added to 1 mL of enzyme solution, and 1 mL of distilled water was used to replace enzyme solution for control. The absorbance of the reaction solution was measured at 290 nm before the reaction. Then the solution was kept in a constant temperature water bath at 30°C for 0.5 h, and the absorbance of the reaction solution was measured. The amount of enzyme required to change the absorbance value of 0.01 every 5 min before and after the reaction was defined as a unit (U). Cell enzyme activity was expressed in enzyme units per gram of wet cells (U g^{-1}).

Experiment S5. The total phenols

2 mL of tobacco suspension culture cells was mixed with 10 mL ethyl acetate, then sonicated and statically extracted for 2 h. The ethyl acetate extract was dried naturally in a flow hood, and the residue was dissolved in 3 mL of 75% ethanol. The absorbance was measured at 280 nm, with 3 mL of 75% ethanol as the control, salicylic acid as the standard, and the absorbance of 1 μg salicylic acid at 280 nm representing one unit of phenol accumulation.[4]

Experiment S6. Catalase (CAT) activity

Tobacco cells of 0.1 g was suspended in 3 mL of phosphate buffer (50 mM, pH 7.8), followed by the addition of 0.1 M H_2O_2 solution. And then, the time was immediately counted, and the absorbance was measured at 240 nm per minute. The measurement repeated 3 times, each as A_1, A_2, A_3. For the control A_0, cells were treated in boiling water for 10 min and the absorbance was measured at the same condition. ΔA_{240}

represented the change of CAT activity, and the calculation formula was:[5] $\Delta A_{240}=A_0-(A_1+A_2+A_3)/3$.

Experiment S7. The Glucose-6-phosphate dehydrogenase (G6PDH)

The activity of G6PDH was determined by measuring nicotinamide adenine dinucleotide phosphate (NADPH), the catalytic product of G6PDH. 3 mL of suspension cells were centrifuged to remove the supernatant, and 0.5 g PVP was added. Then 1 mL pre-cooled enzyme extract (containing 0.42 mol L^{-1} mannitol, 0.005 mol L^{-1} KCl, 0.005 mol L^{-1} $MgS0_4$, 0.05 mol L^{-1} Tris-HCl) and quartz sand were ground on ice. The grinding solution was transferred to a 5 mL centrifuge tube, and centrifuged at 10,000 × g for 15 min. The supernatant was taking as the crude enzyme extract. 0.1 mL enzyme solution was incubated with a mixed solution (0.09 mol L^{-1} G-6-P-2Na, 0.003 mol L^{-1} NADP, 12.5 mmol L^{-1} $MgCl_2$, 0.05 mol L^{-1} Tris-HCl) at 35°C in a water bath for 5 min. Afterwards, the absorbance at 340 nm before and after the reaction was measured using ultraviolet spectrophotometer. The amount of enzyme required to change the absorbance value by 0.01 every 5 min before and after the reaction was defined as a unit U. Cell enzyme activity was expressed in enzyme units per gram of wet cells (U g^{-1}).[6, 7]

Experiment S8. The biomass

Plant cell biomass was calculated based on dry cell weight (DW), and wet cells were air-dried to constant weight at 45°C.

Supplemental Discussion

Discussion S1. Effect of HNTs on tobacco cells

Cells are more sensitive to external substances and react faster. Some reaction signals of nanoparticles can be reflected at the cell level, but not necessarily at the plant level. Therefore, we carried out plant cell exposure experiments in the following section. Tobacco is a common research model to understand in different areas of plant biology such as tissue culture studies and genetic engineering. Tobacco cell and tissue cultures were generally employed for identifying the interactions of plant cells with numerous environmental pollutants including nanoparticles.[8, 9] The effect of HNTs on the viability of tobacco cells was investigated by the TTC method. As shown in Fig. S1A, HNTs had no obvious toxicity to tobacco cells under 80 μg mL^{-1}, and the cell survival rate was higher than 80%. But at high concentrations (greater than 160 μg mL^{-1}), HNTs showed significant toxicity to tobacco cells, and the toxicity was time- and dose-dependent. These results are similar to the effect of HNTs on wheat growth in a dose-dependent manner. Considering that when the concentration of HNTs was greater than 80 μg mL^{-1}, the viability of tobacco cells was significantly reduced with the extension of cultivation time. So, the HNT concentration (80 μg mL^{-1}) and its half-diluted HNT concentration (40 μg mL^{-1}) that affected the tobacco cells viability were used for the biochemical properties' studies. As shown in Fig. S1B, the biomass of tobacco cells increased significantly after the addition of low concentration HNTs, suggesting that HNTs in low concentration could stimulate the growth of tobacco cells.

Under normal conditions, the intracellular and extracellular pH of plant suspension cells should be kept basically constant. However, when stressed by external factors, such as elicitors, the cytoplasm will be acidified.[10] The alkalization of plant cell culture

media was considered to be the initial marker event of plant defense response. As a result of the ion exchange inside and outside the cell, the culture medium will be alkalized accordingly. As shown in the Fig. S1C, after giving low doses of HNTs for 1 h, the pH of the cell culture medium increased significantly, indicating that the tobacco cells culture medium alkalized by the induction of HNTs. The result indicates that HNTs activated the ion pump of the tobacco cell membrane. This is the first sign of the defense response of plants.

The phenylpropane metabolic pathway is an important biochemical pathway for the defense reaction of plants and the formation of secondary metabolites, such as the formation of phytoalexins. It is involved in the synthesis of phenol, benzoic acid, plant signal molecule salicylic acid and a series of compounds related to plant defense response. PAL is a key enzyme in the metabolic pathway of phenylpropane and also a symbolic enzyme in plant defense reactions.[11] The result in Fig. S1E showed that the PAL activity in plant cells increased first and then decreased after the addition of HNTs, reaching the maximum value at 24 h, which was 2.18 times higher than that of the control group. This suggested that HNTs could stimulate cell defense response, PAL activity, and promote phenolics accumulation. Phenolic compounds in plants are an important compound closely related to the defense response of plants. A proper concentration of phenol in the cell is beneficial to the accumulation of secondary metabolites. Some phenolic compounds form lignin through gathering, thicken cell walls, and improve plant disease resistance through lignin.[12] In addition, phenols are antioxidants, which can reduce the harmful effects of reactive oxygen molecules

produced in defense reactions on cells. The synthesis of phenol precursors is catalyzed by PAL enzyme, so the change of PAL enzyme activity ultimately affects the accumulation of phenol. Fig. S1D showed that the addition of HNTs could effectively increase the accumulation of phenolics.

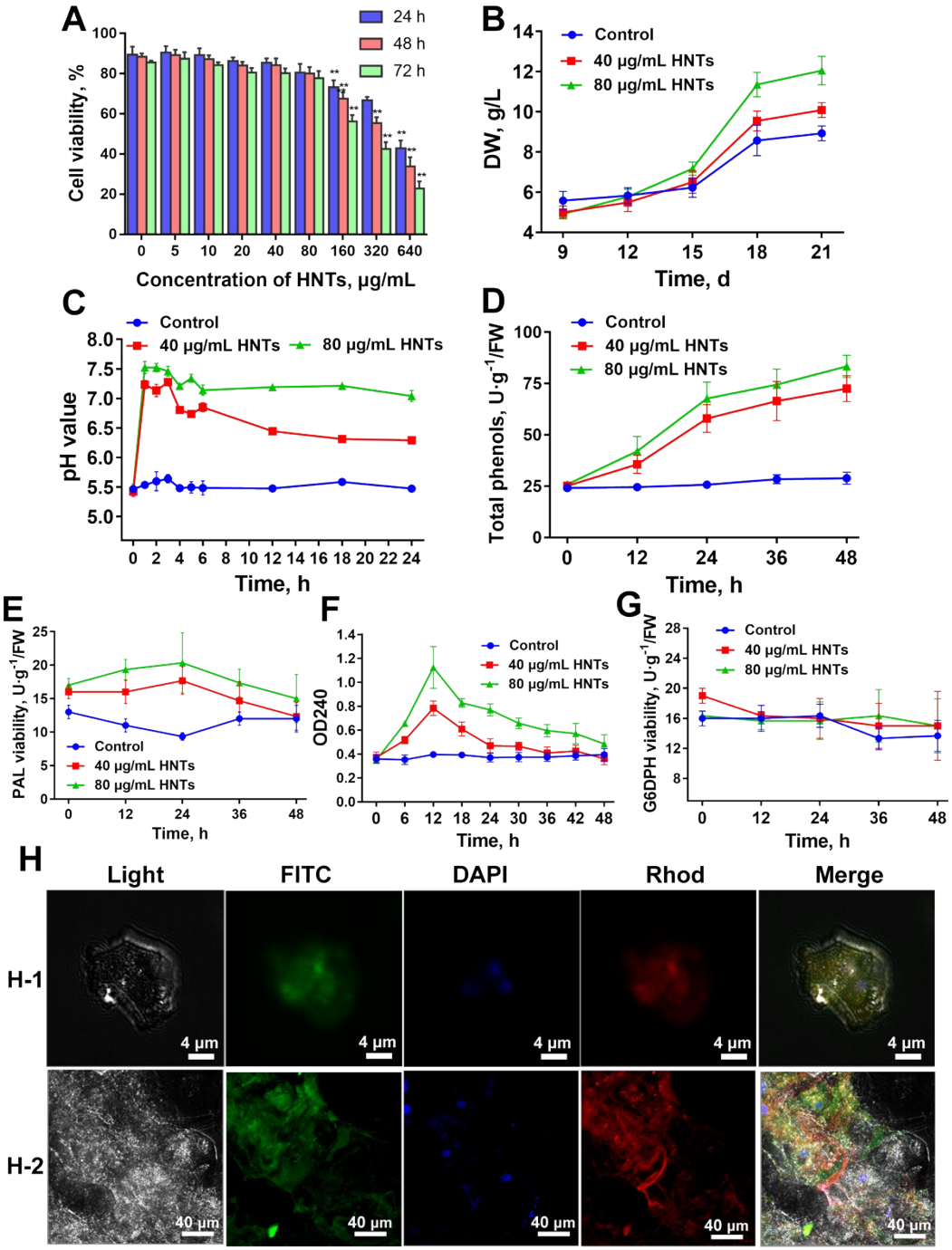

Fig. S1. Effect of HNTs on the growth and biochemical properties of tobacco cells. (A. Cell

viability at 24, 48 and 72 h, *P<0.05, **P<0.01. B. The biomass. C. pH of culture medium. D. Total phenols. E. PAL activity. F. CAT activity. G. G6PDH activity. H. Observation of HNTs uptake by tobacco cells with laser confocal microscope; H-1: laser confocal microscope map of single cell; H-2: laser confocal microscope map of multiple cells; Light: laser confocal microscope map of tobacco cells under natural light source; FITC: laser confocal microscope map of FITC-labeled HNTs co-cultured with tobacco cells; DAPI: laser confocal microscope map after DAPI staining the nucleus of tobacco cells; Rhod: laser confocal microscope map of tobacco cytoskeleton stained by Rhod; Merge: Overlapping the above four maps, it was found that HNTs existed in the nucleus, cytoskeleton and other parts of tobacco cells.

Catalase is widely distributed in plant cells and belongs to active oxygen scavengers. It can decompose the active oxygen generated in the body's metabolism, such as hydrogen peroxide and superoxide anion.[13] These substances have a toxic effect on the body, especially the plasma membrane. CAT activity is closely related to the physiological activities of plants such as stress resistance, cold resistance, disease resistance and regulation of cell apoptosis.[14] The results showed that after the addition of HNTs, with the extension of the treatment time, the CAT activity of cells showed a trend of first increasing and then decreasing. Fig. S1F showed that when low concentrations of HNTs were used to treat plant cells, they stimulated the plant cell's resistance to stress, and responded to environmental stresses through changes in cell CAT activity.

G6PDH (EC 1.1.1.49) is widely present in animals, plants, microorganisms and cultured cells. It is a key enzyme in the pentose phosphate pathway. It catalyzes the

oxidation of 6-phosphoglucose to 6-phosphogluconolactone and at the same time reduces NADP + to NADPH. It plays an important role in metabolite biosynthesis and maintaining the reducing capability of cells. Therefore, the activity of glucose 6-phosphate dehydrogenase can reflect to a certain extent in metabolite biosynthesis and the antioxidant capacity of the body. The activity of G6PDH was determined by measuring NADPH, the catalytic product of G6PDH.[15, 16] As shown in the Fig. S1G, after treatment with HNTs, the trend of G6PDH activity was not significantly different from the control. Therefore, HNTs might not play a role in G6PDH. Fig. S1H show the laser confocal microscope images of tobacco cells treated by HNTs. The FITC labeled HNTs was observed in the nucleus, cytoskeleton and other parts of tobacco cells, suggesting HNTs pass the cell membranes and entered the plant cells.

Reference

1. J. Iborra, J. Guardiola, S. Montaner, M. Cánovas and A. Manjón, 2, 3, 5-Triphenyltetrazolium chloride as a viability assay for immobilized plant cells, *Biotechnology Techniques*, 1992, **6**, 319-322.

2. L. A. Castro-Concha, R. M. Escobedo and M. L. de Miranda-Ham, in *Plant Cell Culture Protocols*, Springer, 2006, 71-76.

3. A. Pina and P. Errea, Differential induction of phenylalanine ammonia-lyase gene expression in response to in vitro callus unions of Prunus spp, *Journal of Plant Physiology*, 2008, **165**, 705-714.

4. Y. Angelova, S. Petkova, E. Zozikova, E. Kotseva and L. Iliev, Effects of kinetin

and 4PU-30 on the growth and the content of polyphenols in tobacco callus tissue, *Bulgarian Journal of Plant Physiology*, 2001, **27**, 36-42.

5. M. Zacchini and M. de Agazio, Spread of oxidative damage and antioxidative response through cell layers of tobacco callus after UV-C treatment, *Plant Physiology and Biochemistry*, 2004, **42**, 445-450.

6. X. Wang, Y. Ma, C. Huang, Q. Wan, N. Li and Y. Bi, Glucose-6-phosphate dehydrogenase plays a central role in modulating reduced glutathione levels in reed callus under salt stress, *Planta*, 2008, **227**, 611-623.

7. V. Hadačová, M. Kamínek and J. Luštinec, Glucose-6-phosphate dehydrogenase in tobacco callus strains differing in their growth and their requirement for auxin and cytokinin, *Biologia Plantarum*, 1975, **17**, 448-451.

8. C. Ritzenthaler, A. Nebenführ, A. Movafeghi, C. Stussi-Garaud, L. Behnia, P. Pimpl, L. A. Staehelin and D. G. Robinson, Reevaluation of the effects of brefeldin A on plant cells using tobacco Bright Yellow 2 cells expressing Golgi-targeted green fluorescent protein and COPI antisera, *The Plant Cell*, 2002, **14**, 237-261.

9. S. Mahjouri, M. Kosari-Nasab, E. M. Kazemi, B. Divband and A. Movafeghi, Effect of Ag-doping on cytotoxicity of SnO2 nanoparticles in tobacco cell cultures, *Journal of Hazardous Materials*, 2020, **381**, 121012.

10. E. O'Sullivan and S. Condon, Intracellular pH is a major factor in the induction of tolerance to acid and other stresses in Lactococcus lactis, *Applied and Environmental Microbiology*, 1997, **63**, 4210-4215.

11. J. Zhao, L. C. Davis and R. Verpoorte, Elicitor signal transduction leading to

production of plant secondary metabolites, *Biotechnology advances*, 2005, **23**, 283-333.

12. O. Daniel, M. S. Meier, J. Schlatter and P. Frischknecht, Selected phenolic compounds in cultivated plants: ecologic functions, health implications, and modulation by pesticides, *Environmental Health Perspectives*, 1999, **107**, 109-114.

13. E. A. Havir and N. A. McHale, Biochemical and developmental characterization of multiple forms of catalase in tobacco leaves, *Plant Physiology*, 1987, **84**, 450-455.

14. A. Sofo, A. Scopa, M. Nuzzaci and A. Vitti, Ascorbate peroxidase and catalase activities and their genetic regulation in plants subjected to drought and salinity stresses, *International Journal of Molecular Sciences*, 2015, **16**, 13561-13578.

15. S. Esposito, Nitrogen assimilation, abiotic stress and glucose 6-phosphate dehydrogenase: The full circle of reductants, *Plants*, 2016, **5**, 24.

16. S. Landi, R. Nurcato, A. De Lillo, M. Lentini, S. Grillo and S. Esposito, Glucose-6-phosphate dehydrogenase plays a central role in the response of tomato (Solanum lycopersicum) plants to short and long-term drought, *Plant Physiology and Biochemistry*, 2016, **105**, 79-89.